HHS Public Access

Author manuscript

Int Mech Eng Congress Expo. Author manuscript; available in PMC 2015 July 17.

Published in final edited form as:

Int Mech Eng Congress Expo. 2012 November ; 2: 493–501. doi:10.1115/IMECE2012-88081.

Third-Order Muscle Models: The Role of Oscillatory Behavior In Force Control

Davide Piovesan,
Rehab. Institute of Chicago, Chicago, IL, USA

Alberto Pierobon, and
Brandeis University, Waltham, MA, USA

Ferdinando A. Mussa-Ivaldi
Northwestern University, Chicago, IL, USA

Abstract

This paper presents the analysis of a third-order linear differential equation representing a muscle-tendon system, including the identification of critical damping conditions.

We analytically verified that this model is required for a faithful representation of muscle-skeletal muscles and provided numerical examples using the biomechanical properties of muscles and tendon reported in the literature.

We proved the existence of a theoretical threshold for the ratio between tendon and muscle stiffness above which critical damping can never be achieved, thus resulting in an oscillatory free response of the system, independently of the value of the damping. Oscillation of the limb can be compensated only by active control, which requires creating an internal model of the limb mechanics.

We demonstrated that, when admissible, over-damping of the muscle-tendon system occurs for damping values included within a finite interval between two separate critical limits. The same interval is a semi-infinite region in second-order models. Moreover, an increase in damping beyond the second critical point rapidly brings the system to mechanical instability.

Introduction

One's ability to exert controlled forces on the environment, such as when manipulating fragile objects, is very important in everyday life. This suggests that force regulation is a necessary component of motor control.

Classical force controllers are generally implemented in systems with small contact impedance in order to limit the force applied to the end effector by external disturbances. In biological motor systems, as the force generated by the muscle fibers increases, so does the muscle's stiffness. This behavior is directly in contrast with the need to keep the contact impedance low. Compliant tendons act as stabilizing impedance buffers between the force-generating element (muscle) and the environment.

Unlike standard second-order Kelvin-Voigt (KV) models, third-order Poynting-Thomson (PT) models include a tendon elastic element in series with the muscle, making them more adherent to the system's physiology and better suited to the study of force control strategies. However, the presence of the tendon element can generate an oscillatory behavior that needs to be compensated by the controller. Limited literature is available on the mechanical behavior of PT models, especially around critical damping conditions. Using an analytical approach, this work investigates the physiological parameters that influence the region of critical damping of a third-order PT model.

We demonstrate that for parameters included within normal physiological ranges a PT model always exhibits an oscillatory free response; therefore, the force controller implemented by the central nervous system (CNS) is required to cope with such biomechanical constraint through feed-back and feed-forward regulation. This is in agreement with findings previously published by our group that empirically showed the construction of an internal feed-forward model trajectory as part of a force-regulation strategy [1].

Third Order Analytical Model

When studying the motion of a mechanical system, $x(\vec{t})$ is a vector of generalized variations of position coordinates (angles, Cartesian coordinates, etc.). We can define $D^n x$ as the set representing the position coordinates variations and their derivatives with respect to time up to the n^{th} order so that $D^n x = \left(\frac{d^n x}{dt^n}, \ldots, \frac{d^2 x}{dt^2}, \frac{d^1 x}{dt^1}, x\right)$, in general $n \in \mathbf{Q}$ [2].

A mechanical system must comply with the Lagrange–d'Alembert principle so that:

$$M(x,t)\frac{d^2}{dt^2}(\vec{x}(t)) + \vec{\sigma}(D^n x, t) = \vec{g}(D^n x, t) \quad (1)$$

where $M(x, t)$ is the inertial matrix of the system in the chosen coordinate frame, $g(\vec{D}^n x, t)$ is the external force field, and $\sigma(\vec{D}^n x, t)$ is the internal force field generated by the mechanical network [2, 3].

The system depicted in Figure (1A) is commonly known as the Kelvin-Voigt (KV) model and is widely used to represent the mechanical behavior of single degree-of-freedom (DOF) mechanical systems. A KV mechanical model is linear and second-order. The system internal viscoelastic force field $\sigma(D^n x, t)$ is represented by the differential equation:

$$\sigma\left(D^1 x, t\right) = -C_{KV} \cdot \dot{x}(t) - K_{KV} \cdot x(t) \quad (2)$$

Most identification techniques proposed in the literature assume the damping C_{KV} and stiffness K_{KV} to be time-invariant.

A more realistic representation of the muscle-tendon complex separates the physical properties of tendon from those of the muscle fibers. Figure (1B) represents a linear, time-

invariant, third-order system known as the Poynting-Thomson (PT) model. This mechanical network is an extension of the KV model commonly used in muscle models and includes tendon elasticity (Hill-type passive model). The PT model includes two separate elastic elements. The element K^S, in series with the muscle fibers, represents the stiffness of the tendon. The parallel between K^P and C^P represents the stiffness and damping of the muscle fibers.

Equation (1) is a model for a time-variant linear system whose oscillating solutions can be found both in the time and frequency domains by means of classical control theory. Assuming the system is stationary (i.e. the resonant angular frequencies $\omega(t)$ in response to a perturbation of the mechanical system are constant), classical Laplace transform techniques can be used to approach the problem in the frequency domain where Eq. (1) is recast in the form:

$$\mathrm{M}s^2\overrightarrow{\mathrm{X}}(s)+\overrightarrow{\sum}(s)=\overrightarrow{\mathrm{G}}(s) \quad (3)$$

Dividing both members of Eq.(3) by the Laplace transform of the displacement function we can calculate the transfer function of the impulse response, namely:

$$\mathrm{M}s^2+\frac{\overrightarrow{\sum}(s)}{\overrightarrow{\mathrm{X}}(s)}=\frac{\overrightarrow{\mathrm{G}}(s)}{\overrightarrow{\mathrm{X}}(s)}. \quad (4)$$

With reference to the PT model shown in Fig.(1B), we can define the transfer function of the muscle fibers as $Z^P = C^P s + K^P$. The transfer function of the whole model is the transfer function of the series of tendon and muscle fibers:

$$\frac{\sum(s)}{\mathrm{X}(s)}=-\frac{K^S Z^P}{K^S+Z^P}=-\frac{K^S\left(C^P s+K^P\right)}{C^P s+K^P+K^S}. \quad (5)$$

Rearranging Eq.(5) we obtain:

$$\sum(s)=-\frac{K^S C^P}{K^p+K^S}s\mathrm{X}(s)-\frac{K^S K^P}{K^p+K^S}\mathrm{X}(s)-\frac{C^P}{K^p+K^S}s\sum(s) \quad (6)$$

hence, the viscoelastic force of the PT system, expressed in the time domain is in the form:

$$\sigma\left(D^2x,t\right)=-\frac{K^S\cdot C^P}{K^S+K^P}\cdot\dot{x}-\frac{K^S\cdot K^P}{K^S+K^P}\cdot x-\frac{C^P}{K^S+K^P}\cdot\dot{\sigma}\left(D^2x,t\right). \quad (7)$$

During a free response, the external force is null, hence $g(D^n x, t)= 0$. Therefore, Eq.(1) can be rewritten as follows:

$$M \cdot \ddot{x} + \sigma\left(D^n x, t\right) = 0 \quad (8)$$

By simple arithmetic and substituting Eq.(7) in Eq.(8), we can isolate the time derivative $\dot{\sigma}$ of the internal viscoelastic force field σ so that:

$$\dot{\sigma}\left(D^n x, t\right) = \frac{M}{C^P}\left(K^S + K^P\right)\ddot{x}(t) + K^S \cdot \dot{x}(t) + \frac{K^S \cdot K^P}{C^P} \cdot x(t) \quad (9)$$

Furthermore, we can derive both members of (8) with respect to time obtaining:

$$M \cdot \dddot{x} + \dot{\sigma}\left(D^n x, t\right) = 0 \quad (10)$$

Substituting Eq.(9) in Eq.(10) we have the third-order formulation of the PT model [4]:

$$M \cdot \dddot{x} + \frac{M}{C^P}\left(K^S + K^P\right)\ddot{x} + K^S \dot{x} + \frac{K^S \cdot K^P}{C^P} x = 0 \quad (11)$$

System's Oscillatory Behavior

The following substitutions can be applied to Eq.(11):

$$A = \left(K^S + K^P\right); B = K^S; C = K^S \cdot K^P. \quad (12)$$

We can represent the characteristic polynomial of the differential Eq. (11) in the following form:

$$\lambda^3 + \frac{A}{C^P}\lambda^2 + \frac{B}{M}\lambda + \frac{C}{M \cdot C^P} = 0. \quad (13)$$

The solution of the characteristic polynomial can be obtained using Cardano's method. Two auxiliary variables can be defined:

$$\begin{aligned} Q &= -\left(\frac{A}{3C^P}\right)^2 + \frac{B}{3M} \\ R &= -\left(\frac{A}{3C^P}\right)^3 + \frac{AB}{6MC^P} - \frac{C}{2MC^P} \end{aligned} \quad (14)$$

The discriminant $\Delta = Q^3 + R^2$ of the cubic equation can be computed [5]. The sign of the discriminant determines the type of solution for equation (13). The roots of a cubic polynomial can be [4, 5]:

- Three distinct real roots ($\Delta < 0$)
- Three real roots, at least two of which are equal ($\Delta = 0$)
- One real root and two complex conjugate roots ($\Delta > 0$)

We will demonstrate that the sign of the discriminant depends on the ratio between the tendon stiffness K^S and the muscle stiffness K^P. A PT model presents an oscillating free response only if the solution of (12) includes a complex root, i.e. if $\Delta > 0$ (see Fig.2).

From Eq.(14), the discriminant can be expressed as a function of the muscle damping as follows [4]:

$$\Delta(C^P)=Q^3+R^2=\frac{1}{108(C^P)^4M^3}\left(4B^3\left(C^P\right)^4-M\left(A^2B^2+18ABC-27C^2\right)\left(C^P\right)^2+4M^2A^3C\right) \quad (15)$$

By solving Eq.(15) for $\Delta(C^P)\gg 0$ we will find the region in the solution domain where the model presents an oscillating free response. The multiplicative term outside the main parenthesis in Eq.(15) is always positive, and the expression within parenthesis is a bi-quadratic form. Hence, to find the solutions to $\Delta = 0$, we can substitute $(C^P)^2 = v$ and solve the following quadratic equation [4]:

$$\Omega(v)=(4Bv^2-M\left(A^2B^2+18ABC-27C^2\right)v+4M^2A^3C=0 \quad (16)$$

To solve Eq.(16) we can impose the following two conditions [4]:

$$\begin{cases} \Delta_\Omega=M^2(AB-9C)^3(AB-C)\geq 0 \\ (A^2B^2-18ABC-27C^2)\geq 0 \end{cases} \quad (17)$$

The expression (17a) represents the condition of the discriminant of (16) to be non-negative, since $v=\left(C_\theta^P\right)^2\geq 0$. The equation (17b) can be clarified by putting (16) in its monic form:

$$v^2-(v_1+v_2)v+(v_1\cdot v_2)=0 \quad (18)$$

The coefficient of the first degree term needs to have the same sign as the sum of the two solutions (which are both positive since $C^P \geq 0$). Since $M^2 > 0$ and

$$AB-C=\left(K^S+K^P\right)K^S-K^S\cdot K^P=\left(K^S\right)^2>0, \quad (19)$$

the condition expressed in Eq.(17a) is equivalent to the following:

$$(AB-9C)\geq 0, \text{ i.e. } \left(K^S+K^P\right)K^S-9\cdot K^S\cdot K^P\geq 0 \quad (20)$$

Assuming the stiffness of the tendon proportional to the stiffness of the muscle, we can define $K^S = \kappa \cdot K^P$, with $\kappa > 0$. Substituting in Eq.(20) we obtain

$$\kappa(\kappa-8)\left(K^P\right)^2 \geq 0 \iff \kappa \geq 8. \quad (21)$$

This shows that for $\kappa < 8$ Eq.(11) and Eq.(13) have two complex conjugate roots, which translate in a free oscillatory response of the PT system, ***independently of the value of*** C^P. On the other hand, if $\kappa \geq 8$ there exists a finite interval of damping values within which the system does not present an oscillatory free response (see Fig.2).

Conditions for Stability

When the system is under-damped, Eq.(13) always has one real root r_1 and two complex conjugate roots $r_{2,3}$. Using Cardano's methods for the solution of cubic algebraic equations, we can calculate the real root defining the following auxiliary variables [5],

$$\begin{aligned} S &= \sqrt[3]{R+\sqrt{\Delta(C^P)}} \\ T &= \sqrt[3]{R-\sqrt{\Delta(C^P)}} \end{aligned} \quad (22)$$

thus obtaining:

$$r_1 = -\frac{A}{3\cdot C^p} + (S+T) \quad (23)$$

Eq.(13) can be recast using the following polynomial decomposition:

$$P(\lambda) = (\lambda - r_1)(\lambda^2 + (\frac{A}{C^P} + r_1)\lambda + \frac{B}{M} + \frac{A}{C^P}r_1 + r_1^2) = (\lambda - r_1)(\lambda^2 + 2\xi\omega\lambda + \omega_n^2) \quad (24)$$

Where

$$2\xi\omega_n = \frac{A}{C^P} + r_1; \omega_n^2 = \frac{B}{M} + \frac{A}{C^P}r_1 + r_1^2 \quad (25)$$

were obtained using Ruffini's rule [6]. By solving the second order term of Eq.(24), the complex roots of the polynomial $P(\lambda)$ are as follows:

$$r_{2,3} = -\frac{\frac{A}{C^P}+r_1}{2} \pm \frac{1}{2}\sqrt{\left(\frac{A}{C^P}\right)^2 - 2\cdot\frac{A}{C^P}r_1 - 4\cdot\frac{B}{M} - 3\cdot r_1^2} = \alpha \pm j\omega \quad (26)$$

Notice that for the system to be stable the real part of all roots (i.e. r_1 and α) needs to be non positive; hence,

$$-\frac{A}{C^P} \leq r_1 \leq 0 \quad (27)$$

Equation (25b) represents the square of the angular natural frequency of the system ω_n^2, which is a parabolic function of the real root r_1. Unlike in a second order system, the natural frequency is a function of the damping.

Stiffness and Length Ratio

The ratio between the tendon and muscle stiffness has been the object of several experimental works. Values of $0.5 < \kappa < 3$ were estimated by Wren and colleagues in several animal studies [7]. For humans, results reported by Loram [8] suggest that $\kappa < 8$ is always true for the soleus and gastrocnemius. Furthermore, it was found that muscles and tendon stiffness are approximately equal for the first dorsal intraosseus muscle (index flexor) at full activation, [9].

Obtaining the ratio κ, either in vivo or in vitro, requires very complex experimental design; however, an approximate estimate can be obtained from the biomechanical parameters of the muscle-tendon system. The stiffness of the tendon can be described as a function of its tissue mechanical properties and geometry [10]:

$$K^S = \frac{A_T E}{L} \quad (28)$$

where A_T is the average cross section of the tendon, E is the elastic modulus and L is its length.

Furthermore, it is reasonable to assume that in order to optimize the modulation of force the muscle would be in the configuration of isometric tetanic contraction. Thus, a similar analytical approach can be taken, where the stiffness of the muscle is [10, 11]:

$$K_0^P = \gamma \frac{P_0}{L_f} \quad (29)$$

Here, $\gamma = 24.5$ is an experimental constant [10], L_f is the length of the muscle fibers and P_0 is the isometric force calculated as $P_0 = PCSA \cdot p_s$, where $PCSA$ is the physiological cross section area, and $p_s = 22.5[N / cm^2]$ is the specific tension of the muscle [10, 12, 13]. Hence, the stiffness ratio can be calculated for each muscle-tendon system based on the biomechanical parameters so that:

$$\kappa = \frac{E}{\gamma \cdot p_s} \frac{A_T}{PCSA} \frac{L_f}{L} \quad (30)$$

Table (1) and Table (2) present the physiological parameters for 5 main muscles across either the wrist or the elbow.

To represent the stiffness in the joint space as the series of an equivalent lumped tendon and muscle, we need to establish the average stiffness ratio between the two elements. Since the force along a single muscle-tendon system is the same for muscle and tendon, we can express the stiffness ratio as the ratio between the elongations of the muscle and the tendon, respectively.

$$P_o = K^P \Delta L_m = K^S \Delta L \Rightarrow \kappa = \frac{\Delta L_m}{\Delta L} \quad (31)$$

Hence, we can lump all muscle-tendon systems acting on the same articulation into an equivalent muscle and equivalent tendon. We assume that the elongation of the equivalent muscle and equivalent tendon are the average of the elongation across the elements that compose them. Thus, the equivalent stiffness ratio at the joint is the average of the stiffness ratios across muscle-tendon systems.

The rotational stiffness of each muscle-tendon system at the joint can be easily calculated starting from the equation of torque τ_0, so that

$$\tau_o = K_\theta \cdot \Delta\theta = P_o \cdot l_m = K \cdot \Delta L_w \cdot l_m = K \cdot (\Delta\theta \cdot l_m) \cdot l_m \Rightarrow K_\theta = K \cdot l_m^2; \quad (32)$$

where K is the stiffness of the specific muscle-tendon system K_θ is the rotational stiffness generated at the joint, ΔL_w is the elongation of the whole muscle-tendon system, l_m is its moment arm, and $\Delta\theta$ is the rotation of the body segment. Assuming that each muscle contributes to the rotational stiffness of the joint on which it acts, we can estimate the lumped joint stiffness by first calculating the equivalent stiffness of the series between each muscle and corresponding tendon and then adding all muscle-tendon stiffnesses (parallel of springs).

Numerical Examples

We validated our result with a numerical example using the biomechanical parameters in Tab.(1) and Tab.(2). The moment arm l_m is calculated for the joint angle $\theta = 0$ where both the wrist and the elbow are completely extended. The equivalent joint stiffness at the wrist are $K_\theta^s = 50.1\ \mathrm{Nm/rad}$ and $K_\theta^P = 18.9\ \mathrm{Nm/rad}$, while at the elbow we obtained $K_\theta^s = 864.8\ \mathrm{Nm/rad}$ and $K_\theta^P = 178\ \mathrm{Nm/rad}$, giving a stiffness ratio of κ_{wrist} = 2.64 and κ_{elbow} = 4.85, respectively. Figure 2 depicts a numerical example for the two joints where κ = 2.64, 4.58, 8, and, 10, using $M_\theta^{wrist} = 0.002\ \mathrm{kg/m^2}$ and $M_\theta^{elbow} = 0.12\ \mathrm{kg/m^2}$ as the value of the inertia with respect to the joints [23].

For $\kappa < 8$ the modulation of C_θ^P does not produce a critical or over-damped condition in neither of the two joints. Furthermore, the values of C_θ^P that eliminate the residual vibration when $\kappa > 8$ are enclosed in a very narrow window. Specifically, for $\kappa = 10$, we obtained $0.366 < C_\theta^P < 0.377$ for the wrist, and $8.694 < C_\theta^P < 8.964$ for the elbow, respectively.

Not only increasing the damping of the system does not attenuate vibration when $\kappa < 8$, but it could also undermine the stability of the system. An increase in damping above the minimum of $\Delta(C^P)$ would increase the value of the real root monotonically to the point of becoming positive (Fig. 3a); thus, making the system unstable. This behavior is quite different from that of a second order system, where the increase of damping would never introduce instabilities.

Figure (3) illustrates how the roots of the characteristic polynomial changes as a function of C^P. The minimum of r_1 (most stable configuration of the system) coincides with the minimum of $\Delta(C^P)$ in Fig.(2). As the damping increases beyond $\Delta(C^P)$, so does r_1.

When taking into account the complex roots $r_{2,3}$ of the specific examples, a (i.e. the real part of the complex roots $r_{2,3}$) is always negative as C^P increases. Furthermore, notice that for $\kappa \geq 8$ the resonant frequency of the system ω (i.e. the value of $r_{2,3}$ imaginary part) is null between the two critical damping values.

Discussion

In this paper we developed a series of analytical tools to investigate the force control of human subject when the muscletendon system is describe as a third-order Poynting-Thomson system. We establish that when the stiffness of the tendon is less than eight times the stiffness of the muscle, the model exhibits an oscillatory free response, independently of the value of the damping. For higher ratios of tendon stiffness to muscle stiffness, the model is over-damped for damping values included within a finite interval between two separate critical limits. Hence, differently from a second-order model, the free response of an over-damped PT model can become oscillatory when the damping is increased.

A numerical example using physiologically compatible values of the muscle-tendon parameters pointed out that the interval of critical damping is quite small. Furthermore, if the damping is increased beyond its higher critical value, the single real root of the PT system increases rapidly to positive values, making the system unstable.

These observations suggest that in physiologically compatible cases the modulation of force is subject to an internal disturbance taking the form of an oscillatory behavior proper of the system's biomechanics.

Given the difficulties of suppressing the internal disturbances using damping, and given that the force generated by the muscle is transmitted to the environment via the tendon in the form

$$\sigma(D^2x, t) = K^S(x(t) - z(t)) \quad (33)$$

we suggest that the control of the oscillations needs to be done indirectly by controlling the position of the muscle-tendon interface $z(t)$. Golgi tendon organs (GTO) are located at the conjunction between muscle and tendon and are normally thought of strain gauges used by the CNS as force transducers. It is possible that their location at the interface ensures a linear

relationship with maximum sensitivity between the tendon's force and elongation, since the tendon is simply an elastic element with constant stiffness, and therefore provide positional information for the controlled variable $z(t)$.

These analytical demonstrations based on a realistic biomechanical model suggest that in order to control their output force, humans need to create an internal model of their mechanics, to compensate for the intrinsic oscillation of the system by actively-varying the length of the tendon. It is plausible that the same control strategy could be used to predict and compensate for externally introduced vibrational disturbances. This would still require the subject to create an internal model of the oscillatory behavior of the limb. Externally induced deterministic disturbance can be of two main types:

1. The power spectral density of the disturbance is concentrated at few specific frequencies. In this case after few cycles the perturbation can be predicted and compensated as demonstrated in [1].
2. The power spectral density of the disturbance is equally distributed on a wide frequency band.

At first glance the latter kind of perturbation seems not predictable: however, writing each frequency component of the disturbance in the form $x_c(t) = X_c \sin(\omega_c \cdot t)$ the power acting on the inertial load of the limb is:

$$\begin{cases} \mathrm{P}_c = F \cdot \dot{x}_c = M \cdot \ddot{x}_c \cdot \dot{x}_c \\ = -MX_c^2\omega_c^3 \sin(\omega_c \cdot t)\cos(\omega_c \cdot t) \\ = -\frac{MX_c^2\omega_c^3}{2}\sin(2 \cdot \omega_c \cdot t) \end{cases} \quad (34)$$

Since the power spectral density is uniformly distributed, the power P_c needs to be equal for each ω_c. Thus, the amplitude X_c of each perturbation component will be bigger for those that have lower angular frequency. Therefore, if position control of the muscle-tendon interface is used as a force-control strategy, where a fixed stiffness is imposed at the end-point, the signals with low frequency and wide amplitude are likely to result in larger force errors and therefore be more easily identified by the subject. This would create only a partial compensation of the disturbance, but since the stiffness of the tendon is constant, it would eliminate the part of the disturbance generating the higher elastic forces.

Conclusion

These results shed some light on the mechanical properties of muscle-tendon systems, confirming that non parametric techniques based on free vibrations are a viable tool to identify the system's properties, since a free oscillating response is physiologically the most common [3, 24-27].

Furthermore, the third-order model of the muscle-tendon system that we presented agrees with our previous results, which have shown the formation of an internal model of external perturbations during force control tasks [1].

Acknowledgments

This work was supported by NINDS 2R01NS035673

References

1. Kolesnikov, M.; Piovesan, D.; Lynch, K.; Mussa-Ivaldi, F. On Force Regulation Strategies in Predictable Environments; Engineering in Medicine and Biology Society (EMBS): Annual International Conference of the IEEE; 2011. p. 4076-4081.1
2. Padovan J, Guo Y. General Response of Viscoelastic Systems Modelled by Fractional Operators. Journal of the Franklin Institute. 1988; 325(2):247–275.
3. Piovesan D, Pierobon A, Dizio P, Lackner JR. Measuring Multi-Joint Stiffness During Single Movements: Numerical Validation of a Novel Time-Frequency Approach. PloS one. 2012; 7(3):e33086. [PubMed: 22448233]
4. Lee G. On Cross Effects of Seismic Respo Ns S of Structures. Engineering Structures. 1998; 20(4-6):503–509.
5. Weisstein, EW. Cubic Formula. From Mathworld--a Wolfram Web Resource. 05/17/2012, http://mathworld.wolfram.com/CubicFormula.html
6. Goodman, L. Synthetic Division. From Mathworld--a Wolfram Web Resource, 05/17/2012, created by Eric W Weisstein. http://mathworld.wolfram.com/SyntheticDivision.html
7. Wren, TaL. A Computational Model for the Adaptation of Muscle and Tendon Length to Average Muscle Length and Minimum Tendon Strain. Journal of Biomechanics. 2003; 36(8):1117–1124. [PubMed: 12831737]
8. Loram ID, Lakie M, Di Giulio I, Maganaris CN. The Consequences of Short-Range Stiffness and Fluctuating Muscle Activity for Proprioception of Postural Joint Rotations: The Relevance to Human Standing. Journal of Neurophysiology. 2009; 102(1):460–74. [PubMed: 19420127]
9. Cook CS, Mcdonagh M. Measurement of Muscle and Tendon Stiffness in Man. european journal of applied physiology. 1996; 72:380–382.
10. Cui L, Perreault EJ, Maas H, Sandercock TG. Modeling Short-Range Stiffness of Feline Lower Hindlimb Muscles. Journal of Biomechanics. 2008; 41(9):1945–1952. [PubMed: 18499113]
11. Walmsley B, Proske U. Comparison of Stiffness of Soleus and Medial Gastrocnemius Muscles in Cats. Journal of Neurophysiology. 1981; 46(2):250–9. [PubMed: 7264713]
12. Maganaris CN, Baltzopoulos V. In Vivo Specific Tension of Human Skeletal Muscle. Journal of applied. 2001; 90:865–872.
13. Sacks D. Architecture of the Hind Limb Muscles of Cats : Functional Sign If Icance. 1982:185–195.
14. Loren GJ, Lieber RL. Tendon Properties Enhance Wrist Muscle Specialization. Journal of Biomechanics. 1995; 28(7):791–799. [PubMed: 7657677]
15. Delp SL, Buchanan S. How Muscle Architecture and Wrist Flexion-Extension Moment Arms Affect Moments. Journal of Biomechanics. 1997; 30(7):705–712. [PubMed: 9239550]
16. Yamaguchi, GT.; Sawa, AGU.; Moran, DW.; Fessler, MJ.; Winters, JM. Appendix: A Survey of Human Musculotendon Actuator Parameters. Springer; New York: 1990. Multiple Muscle Systems: Biomechanics and Movement Organization.
17. Murray WM, Buchanan TS, Delp SL. Scaling of Peak Moment Arms of Elbow Muscles with Upper Extremity Bone Dimensions. Journal of Biomechanics. 2002; 35:19–26. [PubMed: 11747879]
18. Clavert P, Kempf JF, Bonnomet F, Boutemy P, Marcelin L, Kahn JL. Effects of Freezing/Thawing on the Biomechanical Properties of Human Tendons. Surgical and radiologic anatomy : SRA. 2001; 23(4):259–62. [PubMed: 11694971]
19. Ahmad CS, Disipio C, Lester J, Gardner TR, Levine WN, Bigliani LU. Factors Affecting Dropped Biceps Deformity after Tenotomy of the Long Head of the Biceps Tendon. Arthroscopy: The Journal of Arthroscopic & elated Surgery. 2007; 23(5):537–541.

20. Athwal GS, Steinmann SP, Rispoli DM. The Distal Biceps Tendon: Footprint and Relevant Clinical Anatomy. The Journal of hand surgery. 2007; 32(8):1225–9. [PubMed: 17923307]
21. Baumfeld JA, Van Riet RP, Zobitz ME, Eygendaal D, An KN, Steinmann SP. Triceps Tendon Properties and Its Potential as an Autograft. Journal of shoulder and elbow surgery. 2010; 19(5): 697–9. [PubMed: 20413332]
22. Caldwell GE, Chapman AE. The General Distribution Problem: A Physiological Solution Which Includes Antagonism. Human movement science. 1991; 10:355–392.
23. Piovesan D, Pierobon A, Dizio P, Lackner JR. Comparative Analysis of Methods for Estimating Arm Segment Parameters and Joint Torques from Inverse Dynamics. Journal of Biomechanical Engineering. 2011; 133(3):031003. [PubMed: 21303179]
24. Piovesan, D.; Casadio, M.; Mussa-Ivaldi, FA.; Morasso, P. Comparing Two Computational Mechanisms for Explaining Functional Recovery in Robot-Therapy of Stroke Survivors; Biomedical Robotics and Biomechatronics (BioRob): Annual International Conference of the IEEE; 2012. pp
25. Piovesan D, Dizio P, Lackner JR. A New Time-Frequency Approach to Estimate Single Joint Upper Limb Impedance. Engineering in Medicine and Biology Society (EMBS): Annual International Conference of the IEEE. 2009; 1(3):1282–5.
26. Piovesan, D.; Casadio, M.; Mussa-Ivaldi, FA.; Morasso, PG. Multijoint Arm Stiffness During Movements Following Stroke: Implications for Robot Therapy; Rehabilitation Robotics (ICORR), 2011 IEEE International Conference on; 2011. p. 1-7.
27. Piovesan, D.; Casadio, M.; Morasso, P.; Giannoni, P. Influence of Visual Feedback in the Regulation of Arm Stiffness Following Stroke; Engineering in Medicine and Biology Society (EMBS): Annual International Conference of the IEEE; 2011. p. 8239-8242.

Nomenclature

t	time
s	complex number
$x(\vec{t})$, $X(\vec{s})$	generalized co-ordinate and respective Laplace transform
n	degrees of the derivative with respect to time
$\mathbf{Q}$	rational numbers
$D^n x$	set of all the derivatives of $x(\vec{t})$ with respect to t up to the n^{th} degree
KV	2nd order Kelvin-Voigt
PT	3rd Poynting-Thomson system
C_{KV}	damping of a KV System
K_{KV}	stiffness of a KV System
M, M	generalized mass of the arm and respective Laplace transform
C^P	parallel damping of a PT system representing the damping of muscle fibers
K^P	parallel stiffness of a PT system representing the stiffness of muscle fibers
K^S	series stiffness of a PT system representing the stiffness of tendons
θ, $\Delta\theta$	joint angle and its variation

M_θ^{joint}	inertia of the arm segment with respect to the joint.
C_θ^P	parallel damping of a PT system in the rotational case
K_θ^P	parallel stiffness of a PT system in the rotational case
K_θ^s	series stiffness of a PT system in the rotational case
$\sigma(\vec{D}^n x, t), \Sigma(\vec{s})$	generalized internal force field generated by non inertial elements and respective Laplace transform
$g(\vec{D}^n x, t), G(\vec{s})$	generalized external force field and respective Laplace transform
A, B, C	auxiliary coefficients for 3rd order PT differential equation (function of muscles and tendon stiffness)
R, Q, S, T	Cardano's method auxiliary variables
κ	ratio between tendon and muscle's fibers stiffness
$P(\lambda)$	monic 3rd order characteristic polynomial
$\Delta(C^P)$	discriminant of the 3rd order characteristic polynomial
v	auxiliary variable for the discriminant of the characteristic polynomial
$\Omega(v)$	2nd order polynomial representing the discriminant of the characteristic polynomial as function of the auxiliary variable v
Δ_Ω	discriminant of $\Omega(v)$
$r_1, r_{2,3}$	roots of the monic characteristic polynomial $P(\lambda)$
α	real part of $r_{2,3}$ representing the exponential decay rate
ω	imaginary part of $r_{2,3}$ representing the system's resonant angular frequency
j	imaginary unit $\sqrt{-1}$
ξ	damping ratio
ω_n^2	square of the system's natural frequency
z	coordinate at the junction between tendon and muscle
L	tendon length
L_f	muscle fibers length

ΔL_w	elongation of the muscle as a whole (tendon +fibers)
ρ	linear density of the tendon
A_T	Tendon's cross section area
E	Young's modulus of the tendon
$PCSA$	Physiological cross section area of the muscle
P_0	muscle isometric force
p_s	muscle specific tension at the isometric force
l_m	moment arm at 0° degree
ω_c	frequency component of the external disturbance
$\mathbf{P}_c$	power generated by the inertial force at the frequency component of the external disturbance
$x_c(t)$	time-varying position of the inertial load
X_c	amplitude of the inertial load position

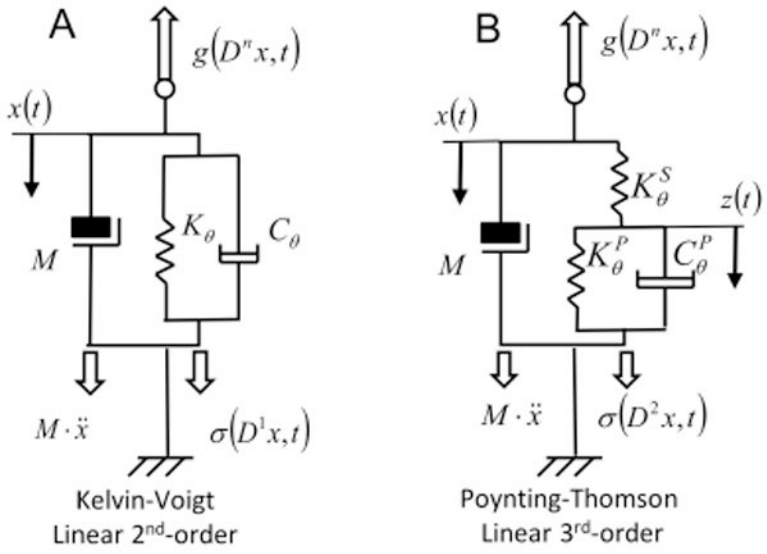

Figure 1.

Mechanical models of muscle-tendon systems. A) Second-order viscoelastic linear system (Kelvin-Voigt). B) third-order viscoelastic linear system (Poynting-Thomson). The schematics highlight the different force fields of the D'Alembert equation - Eq.(1) -. In the figure, each force field is a function of the mechanical elements that generates it.

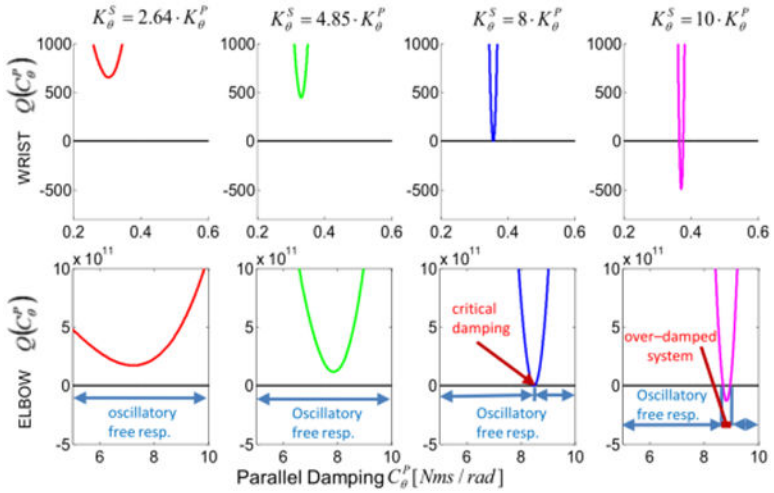

Figure 2.

Sign of the characteristic polynomial's discriminant for a Poynting-Thomson model. The discriminant is shown as a function of the muscle damping C_θ^P and the parameter κ (ratio between the stiffness of the tendon and muscle elements). The function is shown for both wrist and elbow models. For $\kappa < 8$ the discriminant is positive, independently of the value of C_θ^P, which translate to a free oscillatory response of the PT system. If $\kappa \geq 8$ a finite interval of damping values exists within which the system does not present an oscillatory free response.

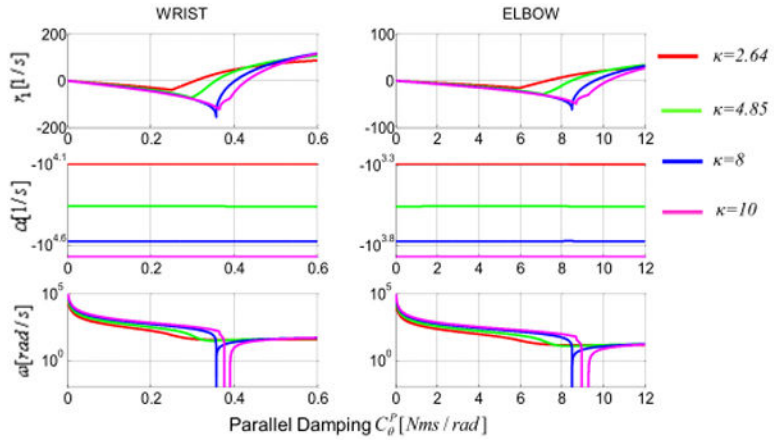

Figure 3.

roots of the characteristic polynomial as function of the damping C^P. First row represents the real root. Second and third rows represent the real and imaginary parts of the two complex conjugate roots. Notice that the imaginary part never changes sign as the damping increases.

Table 1

Extensor Carpii Radialis Brevis (ECRB), Extensor Carpii Radialis Longus (ECRL), Extensor Carpii Ulnaris (ECU), Flexor Carpii Radialis (FCR), Flexor Carpii Ulnaris (FCU)

WRIST	E [Mpa] [14]	A_T [mm^2] [14]	$PCSA$ [cm^2] [14]	L_f [m] [14]	L [m] [14]	$\frac{L_f}{L}$	l_m [cm] [15]	P_o [N]	K_θ^P [Nm/rad]	K_θ^s [Nm/rad]	κ
ECRB	726.1	14.6	2.401	0.071	0.204	0.346	1.60	54.023	4.786	13.303	2.77
ECRL	438.1	14.2	1.300	0.127	0.264	0.476	1.50	29.250	1.267	5.300	4.13
ECU	721.6	15.7	2.100	0.059	0.215	0.272	0.60	47.250	0.709	1.896	2.67
FCR	595.4	17.7	2.119	0.060	0.230	0.259	1.60	47.678	5.001	11.715	2.34
FCU	448.0	27.4	3.636	0.042	0.208	0.202	1.40	81.810	9.376	11.589	1.23

Table 2

Biceps Long Head (BLH), Biceps Short Head (BSH), Triceps Long Head (TLH), Brachialis (BRC), Brachioradialis (BRD)

ELBOW	E [Mpa]	A_T [mm^2]	$PCSA$ [cm^2] [16]	L_f [m] [16]	L [m] [16]*	$\frac{L_f}{L}$	l_m [cm] [17]	P_o [N]	K_θ^P [Nm/rad]	K_θ^s [Nm/rad]	κ
BLH	244.0[18]	63.93[19]	3.330	0.136	0.176	0.771	4.70	74.925	29.816	195.340	6.552
BSH	244.0[18]	48.00[20]	3.220	0.150	0.183	0.821	4.70	72.450	26.140	141.608	5.417
TLH	108.0[21]	143.4 [22]	6.700	0.063	0.249	0.253	2.30	150.750	31.013	32.850	1.059
BRC	176.0**	95.00[22]	9.000	0.090	0.060	1.500	2.60	202.50	37.265	188.379	5.055
BRD	176.0**	46.50[22]	3.000	0.160	0.127	1.260	7.70	67.500	61.282	382.070	6.235

* Values are calculated as the difference between the length of the whole muscle and the length of the fibers.

** Values calculated as the average between all other tendons surrounding the elbow